International Journal of Environmental Sciences
ISSN: 2229-7359
Vol. 11 No. 23s, 2025
https://www.theaspd.com/ijes.php

Biogenic Synthesis Of Cadmium Oxide Nanoparticles: Unlocking New Horizons In Cancer Therapy

Saddam Alwan Resan[1*], Hashim Ali Yusr [2]
[1 ,2] Physics Department, College of Science, University of Wasit, Wasit, Iraq
(saddamalwan7@gmail.com); (hashim@uowasit.edu.iq)
[a] **Corresponding author, Email:** saddamalwan7@gmail.com

Abstract
Cadmium oxide nanoparticles (CdO NPs) were manufactured in an environmentally friendly green method using Hibiscus sabdariffa L. seed extract as a bioreducing and capping agent, and cadmium chloride as the metal precursor. The synthesis process included aqueous extraction, controlled mixing, and alkaline correction, which resulted in a noticeable color change indicating nanoparticle creation. X-ray diffraction (XRD) revealed a polycrystalline structure consisting of cubic CdO and cadmium phases, crystallite sizes ranging from 14.0 to 156.7 nm, and minimal lattice strain, indicating strong crystallinity. Fourier-transform infrared spectroscopy (FT-IR) revealed phytochemical-derived functional groups such as O-H, C≡C/C≡N, C=C/N-H, CH_3, and Cd-O, showing successful surface stabilization. Morphological investigation using atomic force microscopy (AFM) and field emission scanning electron microscopy (FESEM) revealed nanogranular surfaces with moderate roughness and controlled aggregation.Anticancer efficacy against CL-40 colon carcinoma cells, measured by MTT test, revealed outstanding dose-dependent cytotoxicity, lowering cell viability to ~7% at 6.25 µg/mL, with an IC_{50} of 0.7737 µg. The findings suggest that H. sabdariffa-mediated CdO NPs have intriguing structural properties and significant anticancer effectiveness, making them a viable choice for long-term nanomedicine applications.
Keywords: *Cadmium oxide nanoparticles; Hibiscus sabdariffa; Green synthesis; XRD; FT-IR; AFM; FESEM; Anticancer activity; CL-40 cells.*

1. INTRODUCTION

Nanotechnology encompasses a wide spectrum of disciplines, including biological, physical, chemical, and engineering sciences, where advanced techniques are being developed to investigate and manipulate matter at the atomic and molecular scales. Among the various classes of nanomaterials, metallic nanoparticles have attracted significant attention due to their versatile applications in cosmetics, coatings, electronics, packaging, and biotechnology [1].

The overuse and misuse of chemotherapeutic and antibacterial agents have exerted substantial selective pressure, accelerating the emergence of antibiotic-resistant strains [2]. The rapid proliferation of pathogens with resistance to current antibiotics has evolved into a critical public health challenge, thereby emphasizing the urgent need for alternative bactericidal agents [3]. In this context, the synthesis and development of nanoparticles with potent antimicrobial properties represent a promising approach to counteract the escalating threat posed by antibiotic-resistant pathogens, safeguarding both human and animal health [4].

In addition to their antimicrobial potential, biogenic synthesis of nanoparticles—utilizing plant extracts, microorganisms, or other biological systems—has emerged as an environmentally sustainable and biocompatible strategy. In oncology, biogenically synthesized nanoparticles exhibit unique physicochemical and surface properties that can enhance targeted drug delivery, improve cellular uptake, and reduce off-target toxicity. Their ability to generate reactive oxygen species, induce apoptosis, and modulate cellular signaling pathways offers a promising platform for developing novel anticancer therapeutics. Moreover, the eco-friendly nature of green synthesis reduces hazardous byproducts, making it a safer and more sustainable approach for producing nanomaterials with dual antimicrobial and anticancer applications [5-7].

2. Experimental works

Hibiscus (Hibiscus sabdariffa L.) seeds, sourced from the Iraqi market and verified by the Seed Bank of the Iraqi Ministry of Health, were utilized in the synthesis process. The seeds were finely ground using an electric

grinder. A measured quantity of 3 g of the powdered hibiscus was weighed using a precision analytical balance and subsequently added to 100 mL of deionized water. The mixture was subjected to magnetic stirring for 15 min at 60 °C, after which it was allowed to cool to room temperature. The resulting solution was filtered through standard filter paper to remove any residual solid impurities.

Cadmium chloride with a molecular weight of 183.32 g/mol was used as the cadmium source. A quantity of 1.83 g of cadmium chloride was dissolved in 100 mL of deionized water under continuous magnetic stirring until complete dissolution was achieved. The solution was then filtered to remove any insoluble impurities. In parallel, the hibiscus (Hibiscus sabdariffa L.) plant extract was prepared as described previously.

A volume of 20 mL of the plant extract was added dropwise to the cadmium chloride solution, resulting in a slight change in color. Subsequently, sodium hydroxide (NaOH) was prepared at a ratio of 4 g per 100 mL of solution. A measured volume of 3 mL of this NaOH solution was added to the reaction mixture, leading to a gradual color change to a brownish hue. This color transition indicated the formation of cadmium oxide (CdO) nanoparticles, as illustrated in Figure 1.

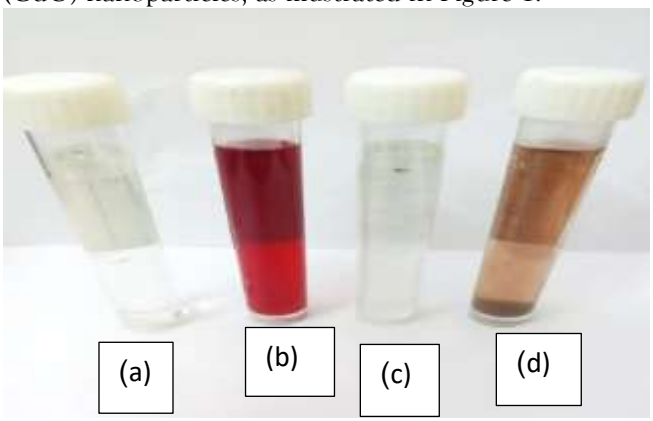

Fig.1. shows (a)deionized water (b) plant extract. (c) cadmium chloride . (d) CdO NPs

3. Results and Discussio

Figure (2) displays the XRD patterns for the CdO film. The peaks consist of cubic face-centered CdO and Cd, which correspond to (111), (200), (102), and (004), along with planes.

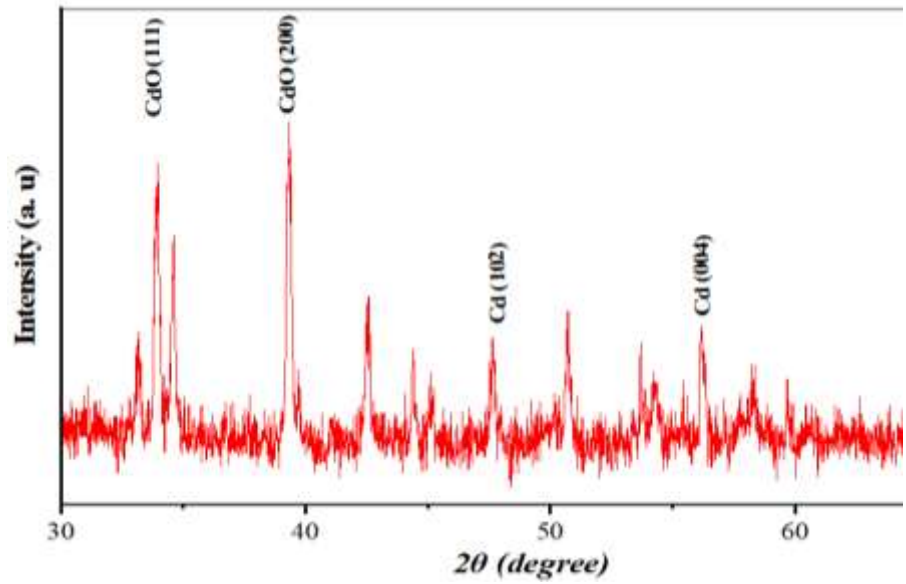

Figure (2) XRD spectrum of Cdo nanostructure

We compared these patterns to standard X-ray diffraction data files (JCPDS file No.00-005-0640 and 00-005-0674) [8]. In Figure 2, you can see how the biosynthesis process with cadmium chloride and an extract from the Hibiscus sabdariffa plant is used to make CdO NPs.

The crystal structure is polycrystalline, and it has both cubic and hexagonal phases. The Bragg peaks are located at 33.97°, 39.33°, and 56.15°, which correspond to the (111) and (200) cubic phases of CdO (JCPDS-05-0640). Some peaks, like those at 47.67° and 66.75°, are caused by the (102) and (004) planes of the cubic phase of the Cd, while the peak at 46.47° is caused by the hexagonal phase of the Cd (102). This study demonstrates that CdO nanoparticle films display a preferred orientation along the (200) diffraction plane. The full width at half maximum (FWHM) of the principal diffraction peaks' intensity and value signifies the creation of diminutive particles. The XRD spectra of the CdO thin film displayed no diffraction peaks suggestive of other phases. The average crystal size D of the 200-plane was determined using the Debye-Scherrer formula, as evidenced by the XRD line broadening shown in Table 1. λ This signifies the X-ray wavelength, θ as the diffraction angle, and β as the full breadth at half maximum. Cadmium oxide (CdO) possesses a face-centered cubic (FCC) crystalline structure.

Table (1) Structural parameters of Cdo nanostructure.

2θ (Degree)	d-spacing (Å)	Height (cts)	FWHM	Crystallite Size (nm)	Micro Strain Lines^{-2}. m^{-4}	Dislocation Density ×(10^{14} lines. m^{-2})
13.68	6.4686	212.08	0.0752	106.5	0.30380	0.88
21.32	4.1648	28.83	0.0981	104.1	0.20000	0.92
25.03	3.5549	84.89	0.1151	93.2	0.19066	1.15
26.54	3.3560	60.59	0.1225	94.2	0.17814	1.13
27.45	3.2465	104.18	0.1042	106	0.15310	0.89
29.40	3.0357	41.33	0.0.226	53.2	0.28518	3.53
33.15	2.7004	25.42	0.2470	50.6	0.26659	3.91
33.91	2.6411	77.27	0.2592	48.3	0.27331	4.29
34.57	2.5925	58.67	0.1978	64.4	0.20120	2.41
39.30	2.2907	98.85	0.2286	60.1	0.19058	2.77
42.50	2.1252	39.59	0.2361	63.7	0.16686	2.46
44.38	2.0394	27.87	0.1184	127.5	0.08000	0.62
45.09	2.0091	21.59	0.0965	156.7	0.06410	0.41
47.62	1.9081	24.62	0.2716	49.5	0.19272	4.08
50.69	1.7995	36.41	0.2134	73.1	0.12309	1.87
54.19	1.6912	14.53	0.7932	19.7	0.42890	25.77
56.18	1.6360	46.80	0.2041	90.3	0.09063	1.23
58.21	1.5837	12.39	0.0907	14.0	0.56500	51.02
59.68	1.5480	14.46	0.1616	108.6	0.07127	0.85
66.75	1.4002	26.70	0.1385	126.1	0.05554	0.63

Nanocrystalline architecture is suggested by crystal sizes. Nanoparticles with low microstrain values have minor lattice distortion, indicating higher structural quality. Cadmium oxide nanoparticles have a straight band gap, face-centered cubic shape, and thermal stability. This arrangement often results in spherical or cubic nanoparticles, depending on the synthesis method. XRD data show nanocrystalline cadmium oxide with FCC symmetry.

Fourier transform infrared spectroscopy (FT-IR) is a valuable device employed to identify the functional groups present in the substance under investigation. Figure (3) illustrates the utilization of the FT-IR spectrum to examine the vibrational patterns of chemical bonds present in CdO nanoparticles. The functional groups were documented in the range of 400-4000 cm^{-1}. When looking at the FT-IR spectra of CdO NPs, prominent peaks can be seen at the following frequencies: 3436.78, 2066.87, 1637.61, 1384.43, and 687.53 cm^{-1}

• Alcohols or adsorbed water are probably the cause of the broad absorption at 3436 cm^{-1}, which is suggestive of hydroxyl (–OH) groups. [9]
• A metal-ligand interaction or the existence of a triple bond, such as C≡C or C≡N, may be indicated by the sharp band at 2066 cm^{-1}.[10]
• In amides, the peak at 1637 cm^{-1} is frequently linked to N–H bending or C=C stretching. [11], [12]
• CH_3 bending vibrations, characteristic of alkyl chains, are indicated by a band at 1384 cm^{-1}.
• The presence of Cd-O bonds, a feature of chlorinated compounds, is confirmed by the strong absorption at 687 cm^{-1}.[13]. Table (2) shows the functional groups, transmittance, and wavenumber.

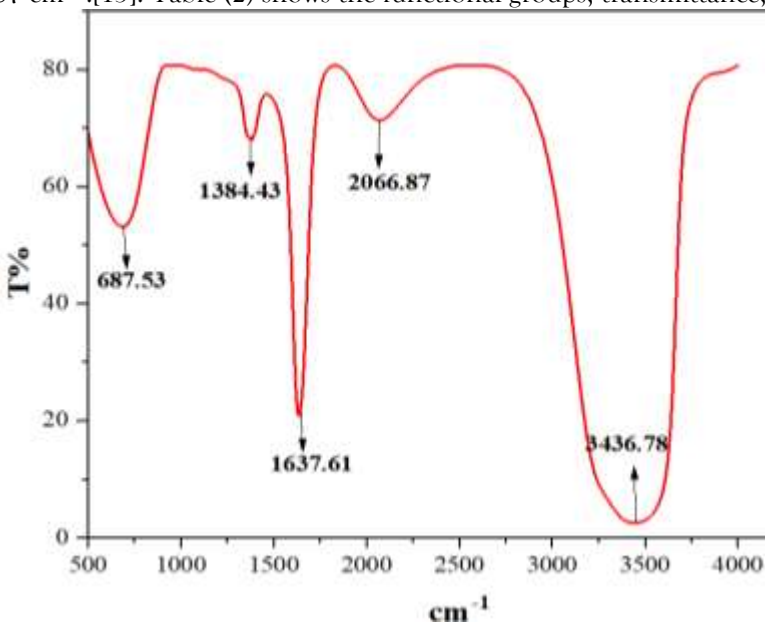

Figure (3) FTIR spectrum for the transmittance of CdO NPs synthesized through biosynthesis methods

Table (2) shows the functional groups, transmittance, and wavenumber

Peak No.	Wavenumber (cm^{-1})	Transmittance (T%)	Functional Group
1	3436.78	2.51	O–H stretch (alcohols, phenols)
2	2066.87	71.29	C≡C or C≡N stretch (alkyne or nitrile)
3	1637.61	20.76	C=C stretch or N–H bend (alkene/amide)
4	1384.43	67.89	CH_3 bending (alkanes)
5	687.53	53.06	Cd–O stretch (alkyl halides)

This 3D AFM picture depicts a granular nanostructured surface characterized by a regular distribution of elevations and depressions. The highest height range attains around 17.4 nm, signifying moderate surface roughness commonly linked to nanostructured materials. The texture is dense and rather isotropic, indicating uniform deposition throughout the synthesis process. This 2D image of the same sample reveals the surface's homogenous grain-like protrusion distribution.

The color map shows height variation like Figure (4), suggesting moderate surface roughness. This image highlights surface morphology's compact granularity.

International Journal of Environmental Sciences
ISSN: 2229-7359
Vol. 11 No. 23s, 2025
https://www.theaspd.com/ijes.php

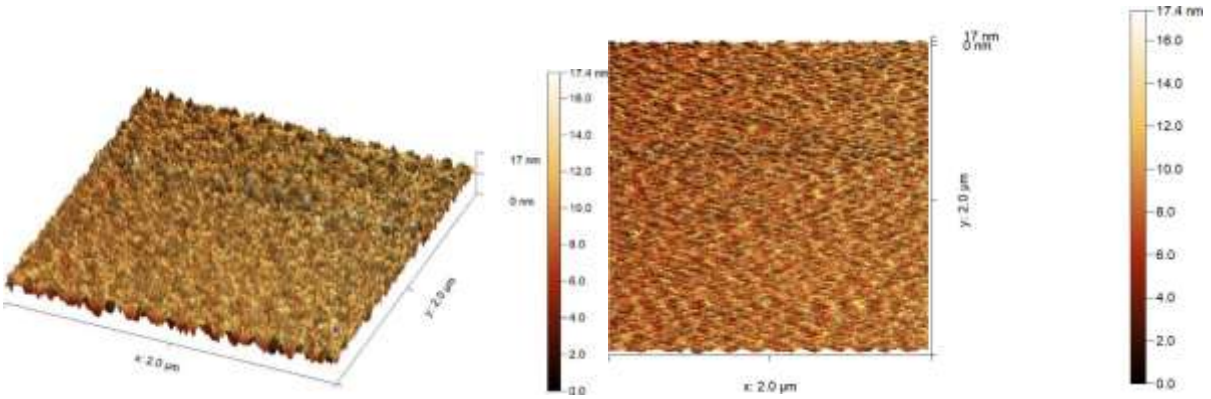

Figure (4) AFM image (2.0 × 2.0 µm²) of CdO NPs

The surface morphology in this enlarged image is more pronounced than in the previous images.The layered or striated structure may indicate crystal alignment or anisotropic development during synthesis.Smoother property transitions and less roughness than in the previous images. This 3D model of the second sample shows elongated ridges.

Height differences may exceed approximately 15 nm, with a smooth surface. Controlled growth conditions or post-synthesis processing may provide flat surfaces. See Figure (5).

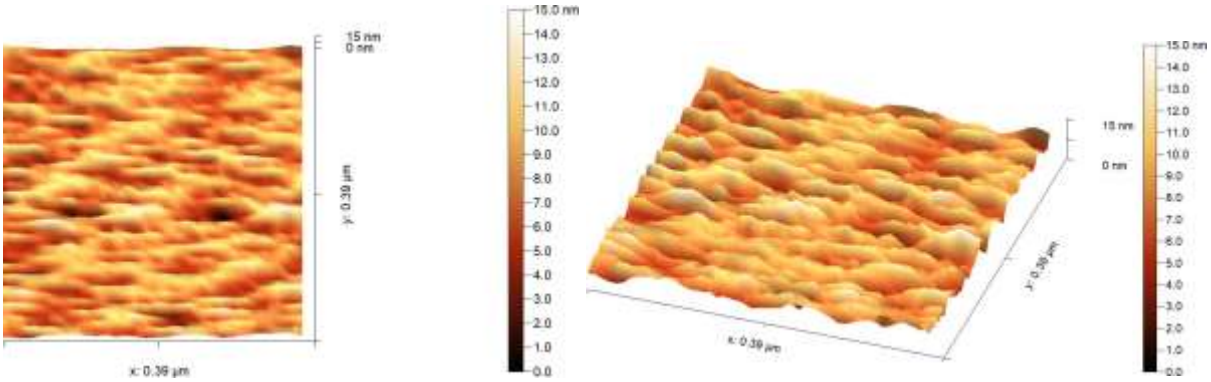

Figure(5) AFM image (0.39 × 0.39 µm²) of CdO NPs

Field Emission Scanning Electron Microscopy (FESEM) images at 1000× magnification reveal different morphological features of nanoparticles deposited on a broken surface.

The image shows a non-uniform structure with conspicuous, huge fissures on the substrate. These fissures could have resulted from drying, sintering, or fast solidification processes. On top of this broken surface, huge agglomerates of irregularly shaped nanoparticles can be seen, indicating considerable particle agglomeration. Nanoparticle sizes range from a few nanometers to tens of micrometers, resulting in dense clusters with irregular edges.

These characteristics indicate that the material was manufactured using chemical or biological techniques, with the synthesis approach (such as green synthesis) possibly impacting the irregular shape. The stark contrast between the broken surface and the dark background suggests a diverse distribution of nanoparticles over the surface, see figure (6).

International Journal of Environmental Sciences
ISSN: 2229-7359
Vol. 11 No. 23s, 2025
https://www.theaspd.com/ijes.php

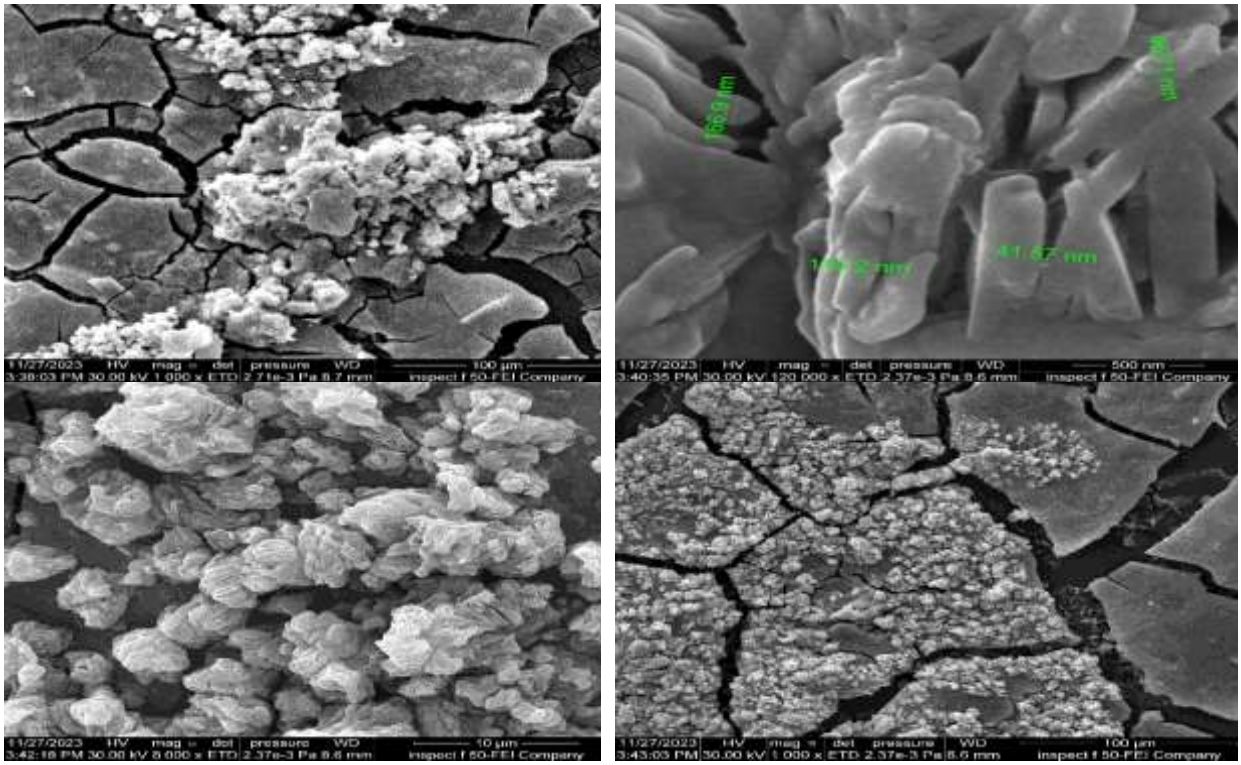

Figure (6) FESEM of CdO NP$_s$ film

4. Anticancer activity

The cytotoxicity of synthesized CdO nanoparticles, derived from Cadmium chlorides, was assessed using the colon carcinoma CL-40 cell line, with a concentration of 1x105 cells per milliliter per well during their exponential growth phase. They were treated with escalating quantities of CdO nanoparticles for 24 hours. Cell viability was measured as a proportion of the untreated control (100% vitality) using the MTT test. The cytotoxicity data for CL-40 cell viability after 24 hours of treatment with varying concentrations of CdO nanoparticles are displayed in table (3). All studies demonstrated a concentration-dependent reduction in cell viability. The CdO nanoparticle solutions significantly reduced CL-40 cell viability in a dose-dependent manner ($P < 0.0001$).For CdO nanoparticles, at a concentration of 0 (without sample), cell viability was 100%, serving as the reference value. At all other concentrations, cell viability declined significantly, reaching levels of 6–9%

Table (3): Cell Viability (mean ± standard deviation (SD) of syntheses CdO NPs treatment on CL-40 cell line.

Dose µg/ml	CdO NP$_s$	
	Mean	SD
0	100	7.64
6.25	7.02	0.35
12.5	7.16	0.35
25	7.57	0.06
50	8.31	1.46
100	7.61	0.75
250	7.02	0.84
500	6.68	1.03

This suggests that the sample exhibits a significantly high toxic effect on the cells, even at low concentrations like 6.25 µg/ml. Refer to figure (7).
CdO NP_s showed high efficacy against cancer cells, with a sharp decrease in light absorption, with an estimated IC_{50} of less than 1µg/ml (0.7737) µg/ml .

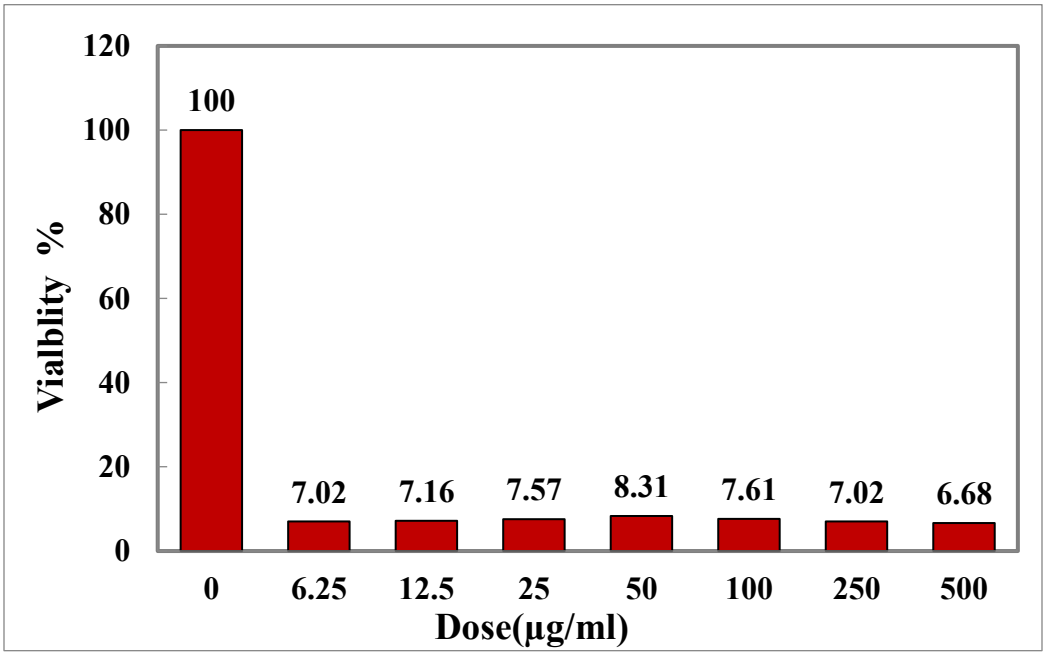

Fig.7. shows the relationship between cell viability with concentration

5. CONCLUSION

The present work, Hibiscus sabdariffa L. seed extract is successfully used to synthesize cadmium oxide nanoparticles in an environmentally acceptable manner. XRD examination revealed that the biosynthesized CdO NPs had a well-defined crystalline structure with little lattice strain, but FT-IR verified phytochemical capping, which may improve stability and biological interactions. Morphological analysis using AFM and FESEM indicated homogenous nanogranular surfaces, moderate roughness, and controlled aggregation, all of which are beneficial for biological applications. The nanoparticles demonstrated remarkable anticancer efficacy against CL-40 colon carcinoma cells, causing significant cell death at low concentrations (IC_{50} of less than 1 µg/mL). This robust bioactivity, together with the environmental friendliness of the green synthesis technique, highlights H. sabdariffa-derived CdO nanoparticles as a prospective platform for future treatment development targeting resistant malignancies.

Conflicts of interest: No conflict of interest among the authors

REFERENCES

1. Rosarin ,F.S. and Mirunalini,S.(2011) Nobel Metallic Nanoparticles with Novel Biomedical Properties, J. Bioanal. Biomed., 3(4), 85-91 .
2. Lee C-R, Cho IH, Jeong BC, Lee SH. Strategies to Minimize Antibiotic Resistance. Int J Environ Res Public Health. 2013;10(9):4274–4305.
3. CLSI. (2011). Performance standard for antimicrobial susceptibility testing; Twenty-First informational supplement. M100-S21.Vol 31 No.(1).
4. Roy,A.S.; Parveen,A.; Kuppakar, A.R.and Prasad, M.N.N.A .(2010). Effect of Nano - Titanium Dioxide with Different Antibiotics against Methicillin-Resistant Staphylococcus aureus.J. Biomaterials and Nanobiotech., 1:37-41.
5. Singh, J., Dutta, T., Kim, K.H., Rawat, M., Samddar, P., Kumar, P. (2018). 'Green' synthesis of metals and their oxide nanoparticles: applications for environmental remediation. *Journal of Nanobiotechnology*,16(1),84.

6. Rajeshkumar, S., & Bharath, L.V. (2017). Mechanism of plant-mediated synthesis of silver nanoparticles – A review on biomolecules involved, characterization, and antibacterial activity. *Chemico-Biological Interactions*, 273, 219–227. Nasrollahzadeh, M., Sajjadi, M., Dadashi, J., Ghafuri, H. (2021). Biogenic synthesis and application of palladium-based nanoparticles. *Green Chemistry*, 23(4), 1312–1356.
7. F. P. Koffyberg, "Diffusion of donors in semiconducting CdO," *Solid State Commun.*, vol. 9, no. 24, pp. 2187–2189, 1971.
8. "Rosmarinus officinalis directed palladium nanoparticle synthesis: Investigation of potential anti-bacterial, anti-fungal and Mizoroki-Heck catalytic activities - ScienceDirect." Accessed: Jan. 29, 2025.
9. AlShourbaji, I., Helian, N., Sun, Y. *et al.* An efficient churn prediction model using gradient boosting machine and metaheuristic optimization. *Sci Rep* 13, 14441 (2023). https://doi.org/10.1038/s41598-023-41093-6
10. Nimma, D., Aarif, M., Pokhriyal, S., Murugan, R., Rao, V. S., & Bala, B. K. (2024, December). Artificial Intelligence Strategies for Optimizing Native Advertising with Deep Learning. In *2024 International Conference on Artificial Intelligence and Quantum Computation-Based Sensor Application (ICAIQSA)* (pp. 1-6). IEEE.
11. Al-Shourbaji, I., Alhameed, M., Katrawi, A., Jeribi, F., Alim, S. (2022). A Comparative Study for Predicting Burned Areas of a Forest Fire Using Soft Computing Techniques. In: Kumar, A., Senatore, S., Gunjan, V.K. (eds) ICDSMLA 2020. Lecture Notes in Electrical Engineering, vol 783. Springer, Singapore. https://doi.org/10.1007/978-981-16-3690-5_22
12. Dash, C., Ansari, M. S. A., Kaur, C., El-Ebiary, Y. A. B., Algani, Y. M. A., & Bala, B. K. (2025, March). Cloud computing visualization for resources allocation in distribution systems. In *AIP Conference Proceedings* (Vol. 3137, No. 1). AIP Publishing.
13. Jameel, Mohammed & Abouhawwash, Mohamed. (2023). A new proximity metric based on optimality conditions for single and multi-objective optimization: Method and validation. Expert Systems with Applications. 241. 122677. 10.1016/j.eswa.2023.122677.
14. Kumar, A. P., Fatma, G., Sarwar, S., & Punithaasree, K. S. (2025, January). Adaptive Learning Systems for English Language Education based on AI-Driven System. In *2025 International Conference on Intelligent Systems and Computational Networks (ICISCN)* (pp. 1-5). IEEE.
15. Wang, Shuang & Hussien, Ganna & Kumar, Sumit & Alshourbaji, Ibrahim & A.Hashim, Fatma. (2023). A modified Smell Agent Optimization for Global Optimization and Industrial Engineering Design Problems. Korean Journal of Computational Design and Engineering. 10. 10.1093/jcde/qwad062.
16. Elkady, G., Sayed, A., Priya, S., Nagarjuna, B., Haralayya, B., & Aarif, M. (2024). An Empirical Investigation into the Role of Industry 4.0 Tools in Realizing Sustainable Development Goals with Reference to Fast Moving Consumer Foods Industry. In *Advanced Technologies for Realizing Sustainable Development Goals: 5G, AI, Big Data, Blockchain, and Industry 4.0 Application* (pp. 193-203). Bentham Science Publishers.
17. Al-Shourbaji, I., & Duraibi, S. (2023). IWQP4Net: An Efficient Convolution Neural Network for Irrigation Water Quality Prediction. *Water*, *15*(9), 1657. https://doi.org/10.3390/w15091657
18. Kaur, C., Al Ansari, M. S., Rana, N., Haralayya, B., Rajkumari, Y., & Gayathri, K. C. (2024). A Study Analyzing the Major Determinants of Implementing Internet of Things (IoT) Tools in Delivering Better Healthcare Services Using Regression Analysis. In *Advanced Technologies for Realizing Sustainable Development Goals: 5G, AI, Big Data, Blockchain, and Industry 4.0 Application* (pp. 270-282). Bentham Science Publishers.
19. Alshourbaji, Ibrahim & Jabbari, Abdoh & Rizwan, Shaik & Mehanawi, Mostafa & Mansur, Phiros & Abdalraheem, Mohammed. (2025). An Improved Ant Colony Optimization to Uncover Customer Characteristics for Churn Prediction. Computational Journal of Mathematical and Statistical Sciences. 4. 17-40. 10.21608/cjmss.2024.298501.1059.
20. Alijoyo, F. A., Prabha, B., Aarif, M., Fatma, G., & Rao, V. S. (2024, July). Blockchain-Based Secure Data Sharing Algorithms for Cognitive Decision Management. In *2024 International Conference on Electrical, Computer and Energy Technologies (ICECET* (pp. 1-6). IEEE.
21. Abouhawwash, Mohamed & Jameel, Mohammed & Askar, S.S.. (2023). Multi-Criteria Decision Making Model for Analysis Hydrogen Production for Economic Feasibility and Sustainable Energy. Multicriteria Algorithms with Applications. 1. 31-41. 10.61356/j.mawa.2023.16161.
22. Elkady, G., Sayed, A., Mukherjee, R., Lavanya, D., Banerjee, D., & Aarif, M. (2024). A Critical Investigation into the Impact of Big Data in the Food Supply Chain for Realizing Sustainable Development Goals in Emerging Economies. In *Advanced Technologies for Realizing Sustainable Development Goals: 5G, AI, Big Data, Blockchain, and Industry 4.0 Application* (pp. 204-214). Bentham Science Publishers.
23. Jameel, Mohammed & Abouhawwash, Mohamed. (2023). A Reference Point-Based Evolutionary Algorithm Solves Multi and Many-Objective Optimization Problems: Method and Validation. Computational Intelligence and Neuroscience. 2023. 4387053. 10.1155/2023/4387053.
24. Praveena, K., Misba, M., Kaur, C., Al Ansari, M. S., Vuyyuru, V. A., & Muthuperumal, S. (2024, July). Hybrid MLP-GRU Federated Learning Framework for Industrial Predictive Maintenance. In *2024 Third International Conference on Electrical, Electronics, Information and Communication Technologies (ICEEICT)* (pp. 1-8). IEEE.
25. Alshourbaji, Ibrahim & Kachare, Pramod & Fadlelseed, Sajid & Jabbari, Abdoh & Hussien, Ganna & AL Saqqar, Faisal & Abualigah, Laith & Alameen, Abdalla. (2023). Artificial Ecosystem-Based Optimization with Dwarf Mongoose Optimization for Feature Selection and Global Optimization Problems. International Journal of Computational Intelligence Systems. 16. 10.1007/s44196-023-00279-6.

26. Orosoo, M., Rajkumari, Y., Ramesh, K., Fatma, G., Nagabhaskar, M., Gopi, A., & Rengarajan, M. (2024). Enhancing English Learning Environments Through Real-Time Emotion Detection and Sentiment Analysis. *International Journal of Advanced Computer Science & Applications*, *15*(7).
27. D. V. Puri et al., "LEADNet: Detection of Alzheimer's Disease Using Spatiotemporal EEG Analysis and Low-Complexity CNN," in IEEE Access, vol. 12, pp. 113888-113897, 2024, doi: 10.1109/ACCESS.2024.3435768.
28. Tripathi, M. A., Goswami, I., Haralayya, B., Roja, M. P., Aarif, M., & Kumar, D. (2024). The Role of Big Data Analytics as a Critical Roadmap for Realizing Green Innovation and Competitive Edge and Ecological Performance for Realizing Sustainable Goals. In *Advanced Technologies for Realizing Sustainable Development Goals: 5G, AI, Big Data, Blockchain, and Industry 4.0 Application* (pp. 260-269). Bentham Science Publishers.
29. Z. Movasaghi, S. Rehman, and Dr. I. Ur Rehman, "Fourier Transform Infrared (FTIR) Spectroscopy of Biological Tissues," *Appl. Spectrosc. Rev.*, vol. 43, no. 2, pp. 134–179, Feb. 2008.
30. J. Coates, "Interpretation of Infrared Spectra, A Practical Approach," in *Encyclopedia of Analytical Chemistry*, 2006.
31. Z. Movasaghi, S. Rehman, and I. U. Rehman, "Fourier transform infrared (FTIR) spectroscopy of biological tissues," 2008.
32. S. Kumar, B. Ahmed, A. K. Ojha, J. Das, and A. Kumar, "Facile synthesis of CdO nanorods and exploiting its properties towards supercapacitor electrode materials and low power UV irradiation driven photocatalysis against methylene blue dye," *Mater. Res. Bull.*, vol. 90, pp. 224–231, 2017.